Q. J. R. Meteorol. Soc. (2001), **127**, pp. 869–886

A mass-flux convection scheme for regional and global models

By P. BECHTOLD[1]*, E. BAZILE[2], F. GUICHARD[3], P. MASCART[1] and E. RICHARD[1]

[1]*Laboratoire d'Aérologie, France*
[2]*CNRM-GMAP, Météo France, France*
[3]*CNRM-GMME, Météo France, France*

(Received 11 February 2000; revised 31 October 2000)

SUMMARY

A bulk mass-flux convection parametrization for deep and shallow convection is presented that includes an efficient and straightforward treatment of numerics, moist thermodynamics and convective downdraughts. The scheme is evaluated in a single-column model context for a tropical deep-convective period and a trade-wind cumulus case. Preliminary applications in a global numerical weather-prediction model and a mesoscale model are also discussed.

The results suggest that the present scheme provides reasonable solutions in terms of predicted rainfall, and tropical temperature and moisture structures. The application of the scheme to various scales is supported by the use of a convective available potential energy convective closure that assures a smooth interaction with the large-scale environment and efficiently suppresses conditional instability of the second kind-like spin-up processes on the grid-scale.

Finally, the theoretical and practical limits of the present approach are discussed together with possible future developments.

KEYWORDS: Convection Mass flux Numerical weather prediction

1. INTRODUCTION

It has been well recognized since the 1960s (e.g. Charney and Eliassen 1964; Manabe and Strickler 1964; Kuo 1965; Ooyama 1971; Yanai *et al.* 1973) that cumulus convection is one of the major processes that affects the dynamics and energetics of atmospheric circulation systems. Since then many cumulus parametrization schemes have been developed for numerical weather-prediction (NWP) models and general-circulation models (GCMs), to account for the subgrid-scale release of latent heat and mass transport associated with convective clouds. A non-exhaustive list of these schemes includes e.g. Arakawa and Schubert (1974), Anthes (1977), Kuo and Raymond (1980), Fritsch and Chappell (1980), Bougeault (1985), Betts and Miller (1986), Tiedtke (1989), Gregory and Rowntree (1990), Kain and Fritsch (1990), Emanuel (1991), Donner (1993), Grell (1993), Wang and Randall (1996), Sun and Haines (1996), and Hu (1997). The common point of all cumulus parametrizations is that they aim to diagnose the presence of larger-scale conditions that would support the development of convective activity and, under appropriate conditions, to introduce tendencies for temperature and moisture (and possibly momentum) that would be consistent with the effects of convective activity. In particular, most parametrizations are designed to drive the model atmosphere towards a convectively adjusted state when they activate. This adjusted state is either predefined ('adjustment' schemes), or is computed using a bulk or spectral cloud model and adjusting the atmosphere through mass exchange between the cloud and the environment (mass-flux schemes).

Two necessary characteristics of any convective parametrization are (i) a reasonable set of criteria to determine when convective adjustment should be initiated, and (ii) procedures for determining the characteristics of a final convectively adjusted state. These characteristics can be evaluated in single-column model (SCM) integrations where large-scale forcing tendencies can be specified to vary with time, and where the

* Corresponding author: Laboratoire d'Aérologie UMR UPS/CNRS 5560, Observatoire Midi-Pyrénées, 14 av. Ed. Belin, F-31400, Toulouse, France. e-mail: becp@aero.obs-mip.fr

response of the SCM (convection scheme) to the imposed forcing can be assessed. This strategy is currently pursued by the Global Water and Energy Cycle Experiment Cloud System Study (GCSS) working groups on convection (Moncrieff *et al.* 1997) that aim to evaluate and intercompare convection schemes in the context of SCM runs against experimental data and data from cloud-resolving models (CRMs). As reported in Bechtold *et al.* (2000), the first results of these intercomparisons have already helped to correct physical and numerical shortcomings in several schemes. However, the conclusions that can be drawn from evaluations within this well-controlled framework are also somewhat limited because (i) larger-scale tendencies are prescribed and not allowed to change in response to the parametrized convection, and (ii) long-range forced SCM runs generally differ from corresponding forced CRM runs as SCMs are not able to correctly represent mesoscale convective organization and the associated cloud–radiation interaction.

Additional evaluations of parametrizations need to be done in prognostic three-dimensional (3D) models. In this environment the scheme must actively complement the highly nonlinear interactions between resolved dynamics and other physical parametrizations (i.e. radiation, turbulent mixing, microphysics). In particular, in contrast to the SCM framework, where a parametrization responds to larger-scale forcing without being able to induce larger-scale dynamical tendencies, in a fully prognostic model it must also be able to drive actively an appropriate larger-scale response to convection. In fully prognostic dynamic models, the efficacy of a convection parametrization is often measured by factors such as: (i) does it activate at the right time and place? (ii) does it produce the right amount and area coverage of precipitation? and (iii) does it enhance the predictive skill of its host model?

Of course, there are many ways of evaluating these measures, and the third criterion above, in particular, depends on the needs of the user. For example, from the practical point of view of a weather forecaster, a convection scheme used in a mesoscale model for a 1–2 day forecast provides valuable information if it has skill in predicting the initiation and evolution of convective events, especially if they involve severe convection. In addition, convective parametrization plays a critically important role in the accurate quantitative prediction of rainfall, especially heavy rain episodes, which present a major challenge for forecasters (Fritsch *et al.* 1998). In contrast, for long-range GCM integrations, a convective parametrization may be judged to be successful if it enhances the ability of the model to accurately represent the mean climate and variability of the tropical atmosphere. Because of these seemingly disparate expectations, cumulus parametrizations have been developed typically with a particular application in mind and may contain inherent biases towards that application.

We believe that, beyond the detection of convective activity, a primary purpose of convective parametrization is to mitigate the effects of inappropriate scale selection in a modelling system's representation of deep convection. It might be possible to develop numerically efficient parametrizations that are useful over a broad range of scales and type of applications, in particular if the parametrized convection nudges the model atmosphere towards a reasonable adjusted state and if it activates in a timely manner. In this context a convection parametrization has been developed on the basis of existing schemes, essentially the rather general framework proposed by Kain and Fritsch (1990, 1993).

The paper is organized as follows. We first present a detailed description of the scheme that is intended to be self-consistent and also accessible to non-specialists in convection parametrization. The reader not interested in this part might directly skip to the evaluation section, where the scheme is applied in an SCM context, and where it is compared to data from observations and CRMs. We conclude with a discussion of the

limits of the present approach, its application in mesoscale and global NWP models, and possible future developments.

2. MASS-FLUX EQUATIONS

Briefly, with the aid of the mass-flux approximation the effect of a convective cloud population on its environment can be written (see e.g. Arakawa and Schubert (1974), Gregory and Miller (1989), and Betts (1997) for various derivations)

$$\left.\frac{\partial\overline{\Psi}}{\partial t}\right|_{\text{conv}} = -\frac{1}{\overline{\rho}}\frac{\partial(\overline{\rho}\overline{w'\Psi'})}{\partial z} \tag{1}$$

$$\approx -\frac{1}{\overline{\rho}A}\frac{\partial}{\partial z}\{M^{\text{u}}(\Psi^{\text{u}}-\overline{\Psi})+M^{\text{d}}(\Psi^{\text{d}}-\overline{\Psi})+\tilde{M}(\tilde{\Psi}-\overline{\Psi})\}$$

$$\approx -\frac{1}{\overline{\rho}A}\frac{\partial}{\partial z}\{M^{\text{u}}\Psi^{\text{u}}+M^{\text{d}}\Psi^{\text{d}}-(M^{\text{u}}+M^{\text{d}})\overline{\Psi}\}, \tag{2}$$

where Ψ is a conserved variable, $\overline{\rho}$ is a reference density, $M=\overline{\rho}wA$ is the mass flux (kg s^{-1}), w is the vertical velocity, z is height, and A denotes the horizontal domain (grid size). Overbars denote ensemble mean (horizontal grid mean) values, tildes denote environmental values, and updraught and downdraught values are denoted by superscripts u and d, respectively. Furthermore, describing the mass exchange of the cloud ensemble with its environment by entrainment ϵ and detrainment δ,

$$\frac{\partial}{\partial z}(M^{\text{u}}\Psi^{\text{u}})=\epsilon^{\text{u}}\overline{\Psi}-\delta^{\text{u}}\Psi^{\text{u}}; \quad \frac{\partial}{\partial z}(M^{\text{d}}\Psi^{\text{d}})=\epsilon^{\text{d}}\overline{\Psi}-\delta^{\text{d}}\Psi^{\text{d}}, \tag{3}$$

we obtain the final result

$$\left.\frac{\partial\overline{\Psi}}{\partial t}\right|_{\text{conv}} = \frac{1}{\overline{\rho}A}\left[\frac{\partial}{\partial z}\{(M^{\text{u}}+M^{\text{d}})\overline{\Psi}\}-(\epsilon^{\text{u}}+\epsilon^{\text{d}})\overline{\Psi}+\delta^{\text{u}}\Psi^{\text{u}}+\delta^{\text{d}}\Psi^{\text{d}}\right]. \tag{4}$$

It can be shown that this equation is also valid for non-conserved variables, i.e. temperature or water mixing ratios, as an additional heating/drying term in (1) cancels out with additional source terms in (3).

3. CLOUD MODEL

The ensemble average updraught and downdraught properties in (4) are determined with the aid of a one-dimensional cloud model that consists of a classical steady-state plume convective updraught/downdraught couple. The cloud model is derived from the Kain–Fritsch computer code but is now designed to represent shallow and deep convective clouds that are characterized by their respective cloud radii.

(a) *Key cloud levels*

First, it is useful to define the model cloud and a certain number of important levels in the cloud that will be needed in the following discussion. As illustrated in Fig. 1, the model cloud extends upwards from the lifting condensation level (LCL) of an air parcel with departure level DPL (DPL actually denotes a 60 hPa thick mixed layer) to the cloud-top level (CTL). The level of free convection (LFC) is the level where the updraught becomes positively buoyant with respect to the environment, and the equilibrium temperature level (ETL) is the level where the buoyancy of the

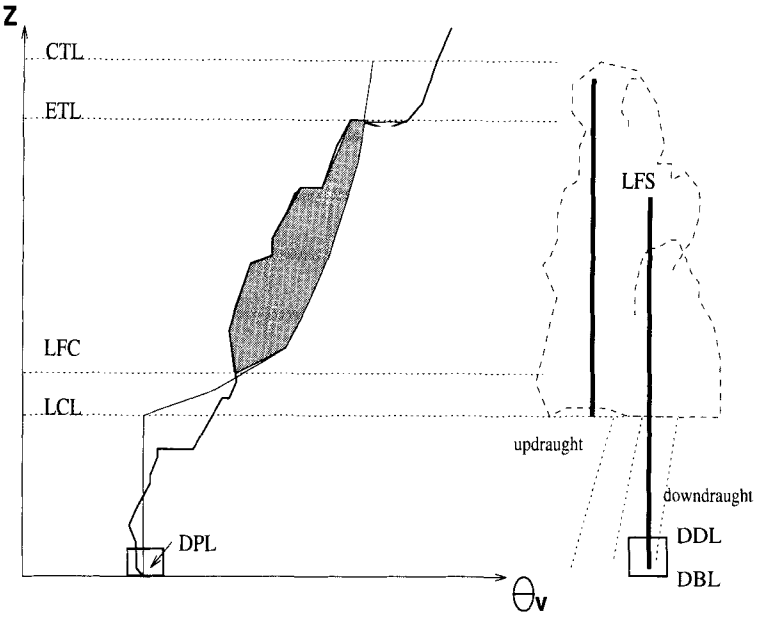

Figure 1. Comparison of Meso-NH SCM runs with CRM including several sensitivity tests: baseline simulation (thick solid line), with cloud radius R_0 of 1000 m (thin solid line with R), without convective downdrafts (thin dashed-dotted line with D), with low vertical resolution (thick dashed-dotted line with Z), and with changed autoconversion of ice in explicit (stratiform) microphysical scheme (thin dotted line with I). The reference CRM run is denoted by the thick dotted line.

updraught drops to zero. The convective available potential energy (CAPE) is defined as the positive area (from the LFC to the ETL) between the in-cloud virtual-potential-temperature sounding and the environmental sounding. The downdraught originates within the cloud at the level of free sink (LFS), and extends down to the downdraught base level (DBL). All downdraught mass is detrained over a fixed layer extending from downdraught detrainment level (DDL) to DBL. Finally, note that the DPL and the DBL are not necessarily equal to the surface level, Fig. 1 serving only as an example.

The following discussion of the different parts of the convection scheme is straightforward in the way that it closely follows the sequential structure of the scheme.

(*b*) *Trigger function*

At present time, the physical processes initiating convection are not well understood. There is no general criterion that tells us when we should allow for convective overturning of the atmosphere; i.e. when we should allow a moist convective parcel to overcome the stable layer at cloud base and to have access to CAPE that is stored aloft due to large-scale forcing associated with e.g. mid-latitude frontal systems, upper-level jets or tropical waves. However, another important issue is the determination of the moist source layer for convection that will be lifted up and will finally determine the properties of the convective cloud (cloud-top level, precipitation, etc.). It turns out that over the tropical ocean this initial moist layer corresponds to the 500 m deep boundary layer (Raymond 1995) and the most difficult problem is to locate the convection. However, in mid-latitude convection, especially at night time, convection might root at upper atmospheric levels.

The numerical formalism is as follows. (Definitions of the various thermodynamic constants and functions are provided in the appendix.) Starting from the ground level, we first construct an at least 60 hPa deep mixed layer with mean potential temperature $\overline{\theta}^{\text{mix}}$ and vapour mixing ratio $\overline{r}_{\text{v}}^{\text{mix}}$. Then this mixed air parcel is lifted without entrainment to its LCL. We directly determine the temperature at the LCL using an algorithm proposed by Davies-Jones (1983), and compute the pressure at the LCL as $P(\text{LCL}) = P_{00}(T(\text{LCL})/\overline{\theta}^{\text{mix}})^{C_{pd}/R_{\text{d}}}$, where P_{00} is the reference pressure. The air parcel is unstable with respect to moist convection if at the LCL

$$\overline{\theta}_{\text{v}}^{\text{mix}} - \overline{\theta}_{\text{v}} + \Delta T/\Pi > 0, \tag{5}$$

with θ_{v} the virtual potential temperature, and with the Exner function defined as $\Pi = (P/P_{00})^{R_{\text{d}}/C_{pd}}$. For deep convection ΔT is intended to crudely trigger/suppress convection as a function of grid-scale motion, where it is defined by $\Delta T = \pm c_w |w_{\text{n}}|^{1/3}$, with $c_w = 6\ \text{K m}^{-1/3}\text{s}^{1/3}$, and where $w_{\text{n}} = A^{1/2}/\Delta x_{\text{ref}}\overline{w}$ is the normalized large-scale vertical velocity using a reference grid space $\Delta x_{\text{ref}} = 25$ km. The sign of ΔT is equal to the sign of w_{n}. Furthermore, we test if the air parcel is able to produce a sufficient cloud depth of 3 km for deep convection by lifting the mixed-layer parcel conserving the equivalent potential temperature $\theta_{\text{e}}(\overline{\theta}^{\text{mix}}, \overline{r}_{\text{v}}^{\text{mix}})$, and searching for the intersection with the environmental saturated curve $\theta_{\text{es}}(\overline{T})$ (see e.g. Raymond 1995). If the air parcel is stable with respect to moist convection, or if its probable cloud thickness is smaller than the specified value, the above procedure is repeated starting at the next higher 60 hPa mixed layer, and so on. For shallow convection we do not use (5) but only the cloud thickness criterion, where shallow clouds are allowed to vary between 500 and 3000 m in depth. The cloud depth is computed based on a small temperature perturbation of 0.2 K of the ascending boundary-layer parcel.

(c) *Updraught*

Updraughts are assumed to originate at the DPL, entrain environmental air in the mixed layer, and then undergo undilute ascent up to the LCL. Starting from the LCL the thermodynamic characteristics of the updraught are computed assuming conservation (except from precipitation processes) of enthalpy or 'liquid-water static energy' h_{il} (see also Emanuel 1994, (4.5.25)) and total-water mixing ratio r_{w}

$$h_{\text{il}} = C_{\text{pm}}T - L_{\text{v}}r_{\text{c}} - L_{\text{s}}r_{\text{i}} + (1 + r_{\text{w}})gz, \tag{6}$$

$$r_{\text{w}} = r_{\text{v}} + r_{\text{c}} + r_{\text{i}}, \tag{7}$$

where the specific heat of moist air is defined as $C_{\text{pm}} = C_{pd} + r_{\text{w}}C_{pv}$, g denotes the gravity constant, and r_{v}, r_{c} and r_{i} denote the mixing ratios of water vapour and non-precipitating cloud water/ice, respectively. The choice of h_{il} is motivated by the fact that it is linear, conserved in the presence of glaciation processes and easily allows glaciation processes to be switched on/off in the model.

The updraught computations are initiated at the LCL using

$$h_{\text{il}}^{\text{u}} = C_{\text{pm}}T(\text{LCL}) + (1 + r_{\text{v}}^{\text{mix}})gz(\text{LCL}),$$

$$r_{\text{w}}^{\text{u}} = r_{\text{v}}^{\text{mix}}.$$

The initial updraught mass flux is set to a unit value of $M^{\text{u}}(\text{LCL}) = \overline{\rho}\, w_{\text{LCL}}\, \pi R_0^2$, with a vertical velocity w_{LCL} of 1 m s^{-1} and an updraught radius R_0 of 1500 m for deep and

TABLE 1. PARAMETERS AND SETTINGS FOR DEEP AND SHALLOW CONVECTION

Parameter	Deep	Shallow
Cloud radius (m)	1500	50
Minimum cloud thickness (m)	3000	500
Adjustment time (h)	$0.5 < \tau < 1$	3
Trigger	$\Delta\theta_v$ + cloud depth	Cloud depth
Downdraught	Yes	No
Precipitation	Yes	No

θ_v is defined in the text.

50 m for shallow convection—all the different parameter switches for deep and shallow convection are summarized in Table 1.

Hereafter we switch to the discretized equations on a vertical model grid k, with k increasing with height. The upstream operator is denoted by

$$\Delta\Psi = \Psi^{k+1} - \Psi^k,$$

layer-mean values are denoted by the additional superscript m. If no superscript is indicated we simply mean the current model level k. Furthermore, it is convenient to denote the entrainment/detrainment rates ϵ and δ in mass-flux units kg s^{-1} instead of units mass flux per length as used in (2)–(4). In this notation the updraught mass flux as well as the updraught values of h_{il} and r_w change through mixing, detrainment and precipitation according to

$$\Delta M^u = \epsilon^{um} - \delta^{um}, \tag{8}$$

$$\Delta(M^u h_{il}^u) = \epsilon^{um}\overline{h}_{il} - \delta^{um}h_{il}^u + M^{u(k+1)}(L_v\Delta r_r + L_s\Delta r_s), \tag{9}$$

$$\Delta(M^u r_w^u) = \epsilon^{um}\overline{r}_w - \delta^{um}r_w^u - M^{u(k+1)}(\Delta r_r + \Delta r_s), \tag{10}$$

where Δr_r and Δr_s are liquid and solid precipitation, respectively. The system (8)–(10) is solved together with a parametrization of microphysics and mixing that are described separately.

(i) *Microphysics and updraught velocity.* The condensate mixing ratios r_c^u, r_i^u are deduced from h_{il}^u and r_w^u using a saturation adjustment, and allowing a gradual glaciation of the cloud in the temperature range between 268 and 248 K (see also Tao *et al.* 1989). The liquid and solid precipitation produced in each model layer is computed following Ogura and Cho (1973)

$$\Delta r_r + \Delta r_s = (r_c^{um} + r_i^{um})\{1 - \exp(-c_{pr}\Delta z/w^{um})\}, \tag{11}$$

where $c_{pr} = 0.02$ s^{-1} is a condensate to precipitation conversion factor. This formulation is essentially based on the fact that in high-speed updraughts precipitation particles do not have time to form or are carried upwards by the draught. The updraught vertical velocity w^u is evaluated with the aid of

$$\Delta\{(w^u)^2\} = \frac{2g}{1+\gamma}\left(\frac{\theta_v^{um} - \overline{\theta}_v^m}{\overline{\theta}_v^m}\right)\Delta z - 2\frac{\epsilon^u}{M^u}(w^u)^2, \tag{12}$$

where $\theta_v = \theta\{1 + (R_v/R_d)r_v\}/(1 + r_w)$, and $\gamma = 0.5$ is the virtual-mass coefficient that approximately takes into account non-hydrostatic pressure perturbations (Kuo and Raymond 1980). The last term of the right-hand side of (12) accounts for zero

environmental momentum. The vertical velocity is also used to compute the CTL, which is defined as the level where $(w^u)^2$ becomes negative. As noted by Carpenter *et al.* (1998), this definition provides the best available estimate of the CTL as the observed values are generally not correlated with the level of neutral buoyancy. Finally, the mass flux is adjusted to decrease linearly between the ETL and the CTL (the detrainment rate becomes proportional to the mass of the model layer), and the total precipitation flux produced by the updraught is obtained by

$$\mathrm{Pr} = \sum_{k=\mathrm{LCL}}^{k=\mathrm{CTL}} (\Delta r_r + \Delta r_s)\, M^u. \tag{13}$$

(ii) *Entrainment and detrainment.* The performance of a plume-cloud model critically depends on the specification of updraught entrainment/detrainment rates which are functions of the cloud radius, and are generally assumed to be constant with height. Following the mixing formalism proposed by Kain and Fritsch (1990), an ensemble of mixed parcels is generated, with positively buoyant parcels supposed to follow the cloudy updraught (entrain) and negatively buoyant parcels supposed to detrain:

$$\epsilon^u = \Delta M_t f_\epsilon, \qquad \delta^u = \Delta M_t f_\delta \tag{14}$$

$$\Delta M_t = M^u c_{etr} \Delta z / R_0, \tag{15}$$

where f_ϵ, f_δ are the fractional entrainment/detrainment rates defined in Kain and Fritsch (1990), and ΔM_t with $c_{etr} = 0.2$ is the total rate at which mass enters the transition region between clear and cloudy air (Simpson 1983).

(*d*) *Downdraught*

In contrast to the updraught computations, where condensate production and glaciation processes are important and therefore h_{il} is a very convenient variable, the downdraught computations become simplified when using the equivalent potential temperature θ_e as it implicitly takes into account the evaporational cooling effect. The definition of θ_e is taken from Bolton (1980) and proved to be highly accurate:

$$\theta_e = T(P_{00}/P)^{R_d/C_{pd}(1-0.28r_v)} \exp\{(3374.6525/T - 2.5403)r_v(1 + 0.81r_v)\}. \tag{16}$$

The downdraught is assumed to be driven by cooling through melting and evaporation of precipitation. It originates at the LFS, defined by the level of minimum environmental saturated θ_e between the LCL and the ETL. The initial values of the downdraught mass flux, θ_e and moisture at the LFS are estimated as

$$M^d(\mathrm{LFS}) = -(1 - \mathrm{Pr_{eff}})\mathrm{M}^u(\mathrm{LCL}), \tag{17}$$

where the precipitation efficiency $\mathrm{Pr_{eff}}$ is given as a function of wind shear and cloud-base height (Zhang and Fritsch 1986). The initial humidity is obtained by mixing updraught and environmental air

$$r_w^d(\mathrm{LFS}) = \chi \bar{r}_w + (1 - \chi) r_w^u; \quad \chi = (\theta_e^u - \bar{\theta}_{es})/(\theta_e^u - \bar{\theta}_e). \tag{18}$$

This definition of the mixed fraction provides a smooth variation of χ. According to (18), the value of θ_e^d at the LFS is set to its saturated environmental value corrected by melting effects, with the cooling due to melting estimated by

$$\Delta T_{melt} = (L_m/C_{ph})\{r_w^u(\mathrm{LCL}) - r_w^u(\mathrm{CTL})\},$$

where $C_{ph} = C_{pd} + r_v C_{pv} + r_c C_\ell + r_i C_s$. This method is motivated by the fact that the amount of downdraught mass flux is dependent on the total downdraught evaporation rate which is not known initially and is itself dependent on the magnitude of the melting effect. We know the amount of solid precipitation but we do not know the amount of ice that is evaporated in the downdraught.

The following equations are used to compute the downdraught properties starting from the LFS down to the DBL which is defined as the level where $\theta_e^d(\text{LFS}) > \bar{\theta}_{es}$.

$$\epsilon^d = -M^d(\text{LFS}) c_{etr} \Delta z / R_0, \quad k > \text{DDL}, \tag{19}$$

$$\delta^d = 0, \quad k > \text{DDL}, \tag{20}$$

$$\Delta M^d = \epsilon^d, \tag{21}$$

$$\Delta(M^d \theta_e^d) = \epsilon^d \bar{\theta}_e, \tag{22}$$

$$\Delta(M^d r_w^d) = \epsilon^d \bar{r}_w. \tag{23}$$

Note that M^d is negative but ϵ^d and δ^d are positive. All downdraught detrainment is assumed to occur over the 60 hPa deep layer DDL–DBL (Fig. 1). For the closure adjustment procedure we will need the values of h_{il}^d. As δ^d is zero everywhere apart from the detrainment layer, we only need to compute the values of h_{il}^d for this layer. It is computed from θ_e^d and r_w^d. The total downdraught evaporation rate is estimated using a specified value of 90% for the relative humidity. If the actual value of humidity in the downdraught in the detrainment layer is less than the specified value, water is evaporated to give the required value. If no water is evaporated, no downdraught is allowed and the downdraught mass flux is set to zero.

(*e*) *Closure*

Finally, a closure assumption is needed to control the intensity of convection. Here we adopt a Fritsch/Chappell-type closure which is based on the assumption that all CAPE in a grid element is removed within an adjustment period τ. For deep convection τ is set to the advective time period $\tau = A^{1/2}/|\mathbf{v}|$, with $\mathbf{v}$ the mean horizontal wind vector between the LCL and the 500 hPa level, and is limited by $0.5 < \tau < 1$ h. The upper limit roughly corresponds to one life cycle of a convective cloud. Following the Betts–Miller scheme, an adjustment time τ of 3 h is used for shallow convection. The final convectively adjusted environmental values can now be computed (see also the main mass-flux equations (4)) using a time integration over τ together with an iterative procedure

$$\begin{aligned}\overline{\Psi}^{(n+1)} = \overline{\Psi}^{(n)} + (\tau/m_t)\{&-\Delta(\tilde{M}^{(n)}\overline{\Psi}^{(n)}) - (\epsilon^{u(n)} + \epsilon^{d(n)})\overline{\Psi}^{(n)} \\ &+ \delta^{u(n)}\Psi^u + \delta^{d(n)}\Psi^d\},\end{aligned} \tag{24}$$

$$\tilde{M} = \bar{\rho}\tilde{w}A, \quad \tilde{w} = \int (\partial\tilde{w}/\partial z)\, dz, \quad \left(\frac{\partial\tilde{w}}{\partial z}\right) = \frac{\epsilon^u + \epsilon^d - \delta^u - \delta^d}{m_t}, \tag{25}$$

where n denotes the iteration number, Ψ stands for either h_{il} or the various water species r_w, r_c, r_i. The total mass of the model layer is denoted by m_t, and $\tilde{M}$ is the compensating environmental mass flux. The essential point of the present adjustment procedure is that only the environmental values $\Psi = h_{il}$, r_w, r_c, r_i are updated and the mass fluxes are adjusted in the closure adjustment procedure, but no updraught or

downdraught computations are repeated so that the updraught and downdraught values of the thermodynamic variables remain unchanged.

Now, computing the new environmental values of θ and r_v from $\overline{h}_{il}$ and $\overline{r}_w$ using (6)–(7), we can compute $\overline{\theta}_e$ and a new value of CAPE by using undilute parcel ascent,

$$\mathrm{CAPE}^{(n+1)} = \int_{\mathrm{LCL}^{(n+1)}}^{\mathrm{ETL}} g \left\{ \frac{\overline{\theta}_e^{(n+1)}(\mathrm{DPL})}{\overline{\theta}_{es}^{(n+1)}} - 1 \right\} \mathrm{d}z, \tag{26}$$

where the new value $\mathrm{LCL}^{(n+1)}$ is obtained from $\overline{\theta}_v^{(n+1)}(\mathrm{DPL})$ by the same procedure as used in the trigger function. The use of the conserved variable $\overline{\theta}_e(\mathrm{DPL})$ instead of θ_v^u in (26) is motivated by the fact that this formulation allows CAPE to be determined directly without executing additional updraught computations.

Then, at all model levels the updraught and downdraught mass fluxes as well as the entrainment/detrainment fluxes and the precipitation flux are multiplied by the adjustment factor

$$F_{\mathrm{adj}}^{(n+1)} = F_{\mathrm{adj}}^{(n)} \frac{\mathrm{CAPE}^{(0)}}{\mathrm{CAPE}^{(0)} - \mathrm{CAPE}^{(n+1)}}, \tag{27}$$

where $\mathrm{CAPE}^{(0)}$ is the initial value of CAPE. The procedure (24)–(27) as described is repeated until $\mathrm{CAPE}^{(n+1)} < 0.1\ \mathrm{CAPE}^{(0)}$. At the end of the adjustment procedure the final convective tendencies are simply evaluated as

$$\left.\frac{\partial \overline{\Psi}}{\partial t}\right|_{\mathrm{conv}} = (\overline{\Psi}^{(n)} - \overline{\Psi}^{(0)})/\tau, \tag{28}$$

where Ψ now stands for either θ, r_v, r_c or r_i.

4. Discussion

The aim was to design a parametrization that incorporates the effects of the essential physics of moist convection while remaining as straightforward and numerically efficient as possible. In adhering to these guidelines, however, it is inevitable that numerous simplifications of real physical processes become necessary. We believe it is important to acknowledge some of these and differences with other schemes.

Steady-state convective-plume models, as used in the present version, neither represent the life cycle of convective clouds nor the horizontal exchange (subsiding motion) between convective clouds. As discussed by Warner (1970) these models tend to overestimate either the cloud vertical velocity (cloud-top height) and/or the upper-level mass flux. However, recent studies (Lin and Arakawa 1997; Cohen 2000) confirm the present approach where the entrainment and detrainment rates are computed as a function of the buoyancy excess of the cloud with respect to the environment. Numerous sensitivity studies suggest that, in spite of the nonlinear set of equations (8)–(15), the present version provides reasonable solutions for both quantities that are only sensitive to the specification of the cloud radius but not to other physical details like the parametrization of precipitation. Finally, the convective adjustment is based on an iteration procedure and does not directly make use of the tendency of CAPE as applied in several updated versions of mass-flux schemes. The adjustment procedure is entirely formulated in conserved variables allowing for a fast convergence of the iteration algorithm.

Physical processes not considered in the present version concern the convective momentum transport. This might lead to errors in long-range global integrations, but promising recent work on this problem (e.g. Kershaw and Gregory 1997) may allow for a realistic inclusion of momentum transports in updated versions of the scheme. Also, we do not explicitly account for mesoscale transports that might give a substantial contribution to the mass flux at upper levels (Donner 1993; Betts 1997; Alexander and Cotton 1998), but the significance of this is largely unknown.

In the following we present SCM numerical experiments in order to assess the sensitivity of the scheme to important parameters (cloud radius, parametrization of downdraughts), and to compare it to observational and numerical data. The SCM experiments have been run with the French community non-hydrostatic research model Meso-NH (Lafore *et al.* 1998).

5. SCM EXPERIMENTS

SCM experiments allow a detailed evaluation of convection schemes against observations and numerical data from CRMs or Large Eddy Simulations (LES). Furthermore, they provide a computationally efficient framework for gauging the behaviour of a parametrization as a function of various specifications of thermodynamic conditions and large-scale tendencies. Thus, SCMs are useful for identifying fundamental deficiencies in a scheme and indicating how robustly parametrizations will perform in fully prognostic 3D models. The GCSS Working Groups 1 and 4 on shallow and deep convective cloud systems (Moncrieff *et al.* 1997) have recently defined a strategy to evaluate convection parametrizations on the basis of SCM runs and compare the results with observations and numerical data. Several intercomparison studies on tropical and continental convection are currently organized (e.g. Bechtold *et al.* 2000). Here we follow this strategy and evaluate the convection parametrization for a deep convective and a shallow cumulus case, using fully prognostic SCM simulations that are forced by observed large-scale horizontal plus vertical advective tendencies.

(*a*) *TOGA-COARE six-day integration*

A six-day period from 00 UTC 20 December to 00 UTC 26 December 1992 of the Tropical Oceans Global Atmosphere (TOGA) Coupled Ocean–Atmosphere Response Experiment (COARE) has been selected as a test case for a tropical oceanic deep convective environment. The precise numerical experiment protocol is described in Krueger *et al.* (1996)*. The case has been run with an SCM version of the Meso-NH model (using the present convection scheme), and a 2D version of a CRM (Redelsperger and Sommeria 1986). The models were forced with observed 'large-scale' tendencies for temperature and water vapour that represent spatial averages over the intensive flux array of 500 × 500 km. The Meso-NH model and the CRM use a stretched vertical grid with resolution varying between 100 m in the boundary layer and 750 m in the upper troposphere. Finally, note that in the present SCM runs, the grid-scale A appearing in the trigger formulation (5) is set equal to the size of the observational domain.

Figure 2 shows the time evolution of the surface precipitation rate as simulated by the Meso-NH SCM and the CRM. The SCM fairly represents the four main convective events with precipitation intensities ranging between 30 and 50 mm d^{-1}. In Fig. 3 are displayed the simulated six-day averaged temperature and moisture biases with

* Available on http://www.met.utah.edu/skrueger/gcss/wg4.html (February 2000).

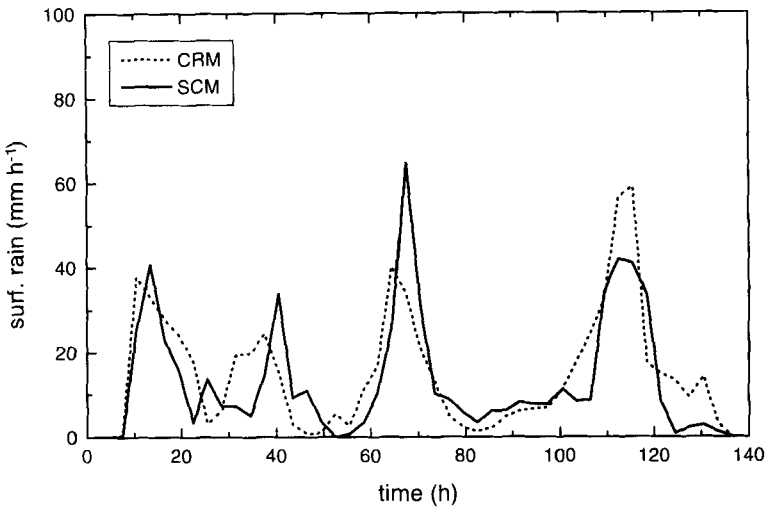

Figure 2. TOGA-COARE six-day case-study starting 00 UTC 20 December 1992. Comparison of Meso-NH single-column model run (solid line) with cloud-resolving model run (dashed line): six-day evolution of surface precipitation intensity.

respect to observations as well as the simulated convective mass fluxes. The Meso-NH baseline simulation produces a cold bias that does not exceed 3 K (compared to 1.5 K for the CRM), and a moisture profile with a maximum bias of 0.6 g kg^{-1} in the lower troposphere but that closely follows the CRM results above 7 km. However, the simulated convective mass flux (Fig. 3(c)) closely reproduces the CRM results. It can be shown, through a comparison with different SCMs (convection schemes), that SCMs generally produce larger temperature biases with respect to observations than corresponding CRM runs, as SCMs cannot represent mesoscale circulations that are part of the total (convective+stratiform) mass flux and the associated cloud–radiation interactions.

In the following we wish to assess how robust the Meso-NH results are with respect to: (i) internal parameters of the convection scheme, such as the parametrization of downdraughts and the cloud radius, and (ii) other model parameters such as the vertical resolution and the stratiform cloud scheme. In this context four additional experiments have been run: an experiment without convective downdraughts, one using a value for the convective cloud radius of 1000 m (instead of 1500 m in the reference run), an experiment with half the vertical resolution of the reference run (corresponding to a grid spacing of 1500 m in the upper troposphere), and an experiment where the precipitation threshold for cloud ice in the stratiform cloud scheme has been set to a value of 0.5 g kg^{-1} (instead of 0.05 g kg^{-1} in the reference run). The results of the sensitivity experiments are also displayed in Fig. 3. It appears that the general shape of the bias and mass-flux profiles is largely unaffected by these changes. However, the largest upper-tropospheric temperature bias and lower-tropospheric moisture bias are observed for the low vertical resolution run. But the upper-tropospheric temperature bias is also significantly affected by changes in the stratiform ice microphysical scheme through an interaction with the radiation scheme. Furthermore, when downdraughts are excluded, the mass flux is overestimated at all levels and the low-level temperature and moisture biases become large. In contrast, the experiment with a cloud radius of 1000 m produces smaller biases in the lower troposphere but a temperature bias that is 1 K larger

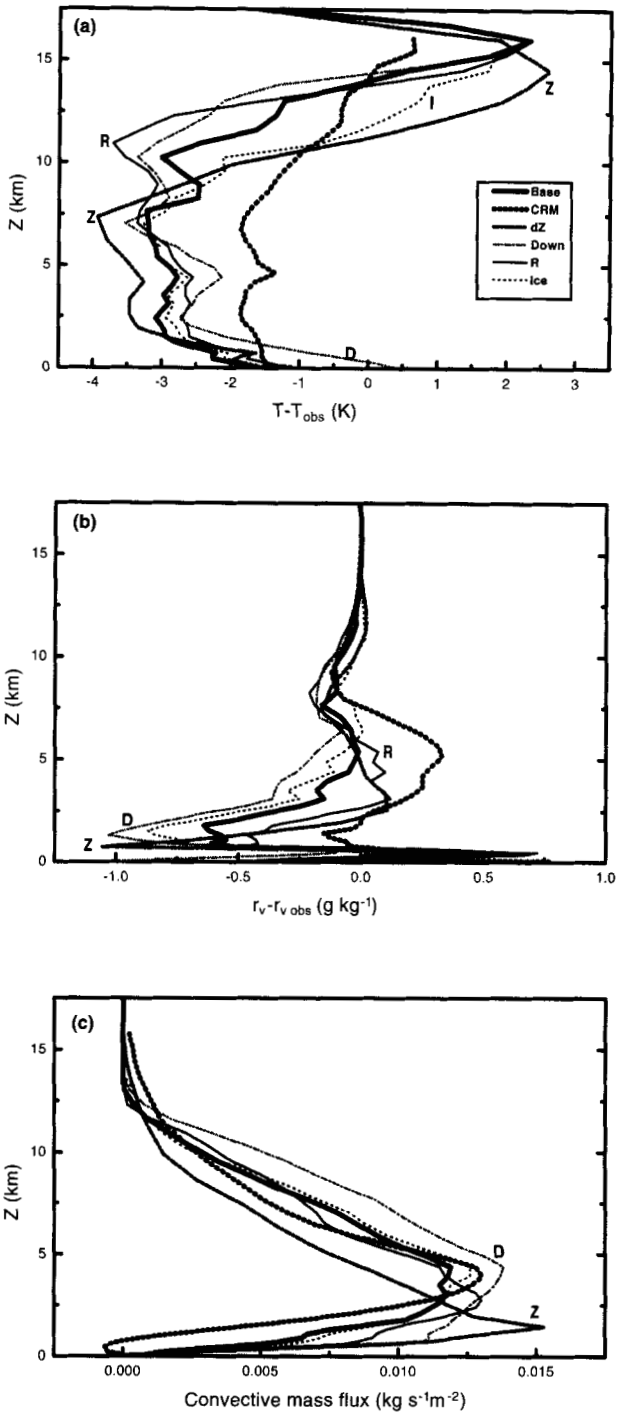

Figure 3. Comparison of Meso-NH single-column model (SCM) runs with cloud-resolving model (CRM) for: differences with respect to observed values of (a) temperature and (b) moisture, and (c) convective mass flux. The different SCM sensitivity tests include: baseline simulation (thick solid line), with cloud radius R_0 of 1000 m (thin solid line labelled R), without convective downdraughts (thin dashed-dotted line labelled D), with low vertical resolution (thick dashed-dotted line labelled Z), and with changed autoconversion of ice in explicit (stratiform) microphysical scheme (thin dotted line labelled I). The reference CRM run is denoted by the thick dotted line.

in the upper troposphere. The present discussion has shown that the scheme performs reasonably robustly in this tropical oceanic environment, but that SCM evaluations of convection parametrizations should focus on profiles of quantities like convective mass flux and moisture bias that are only weakly affected by host-model-dependent physical processes like the interaction between the radiation scheme and the stratiform cloud scheme.

(*b*) *BOMEX shallow cumulus*

The shallow convective part of the scheme is evaluated with the aid of a 9 h integration of a BOMEX* shallow cumulus case using the Meso-NH SCM. The model is forced by a constant-in-time large-scale subsidence, imposed surface fluxes for heat and moisture, and additional tendencies due to radiative cooling and horizontal moisture advection. A detailed discussion of this case, including the numerical protocol and LES results, is given in Siebesma and Cuijpers (1995). The baseline Meso-NH run uses a constant vertical grid spacing of 40 m. Furthermore, sensitivity experiments have been run using a constant vertical grid spacing of 100 m, a convective cloud radius of 100 m, and an experiment labelled 'deep' where convective downdraughts and precipitation processes have been included.

In Fig. 4 we compare the initial temperature/moisture profiles with the simulated profiles after 9 h of integration. The model produces quasi-stationary profiles, but a weak tendency towards stabilization can be observed close to cloud base at 500 m. This is due to a small residual in the boundary-layer budget of the model that is determined by turbulent mixing and convective transport. The mass-flux profiles as produced by the baseline simulation and the different sensitivity experiments are displayed in Fig. 5. The profiles represent time averages over the whole simulation period, and are compared to corresponding LES results (Siebesma and Cuijpers 1995). In general, the different experiments fairly reproduce the LES results, but tend to underestimate the mass flux, especially in the upper half of the cloud layer. The experiment using a cloud radius of 100 m produces the largest upper-level mass flux, but overestimates the top of the cloud layer by about 500 m. On the contrary, the smallest mass-flux values are observed for the experiment labelled 'deep' where the surface precipitation rate attains a value of 1 mm d^{-1}.

It appears that the present parametrization might also be successfully applied to shallow convection, even if a closure based on the moisture budget of the boundary layer might also be attractive. Especially, with the choice of a small 'cloud radius' of 50 m in the entrainment equation (15), a value which is significantly smaller than the actual cloud radius of shallow cumuli, the convection scheme can produce realistic entrainment/detrainment rates for various typical shallow cumulus cases with fractional values of the order of 10^{-3} m^{-1} (see also the discussion of (15) and LES results in Siebesma (1998)). Finally, note that in contrast to deep convective clouds where high values of CAPE are produced by large-scale lifting, shallow convective clouds have low values of CAPE (typically 100–200 J kg^{-1}) that are produced by surface fluxes and subsequent turbulent mixing. The present CAPE closure assures an equilibrium between convective destabilization through surface fluxes and consumption of CAPE by shallow convective clouds that transfer enthalpy and moisture upwards.

* Barbados Oceanographic and Meteorological EXperiment.

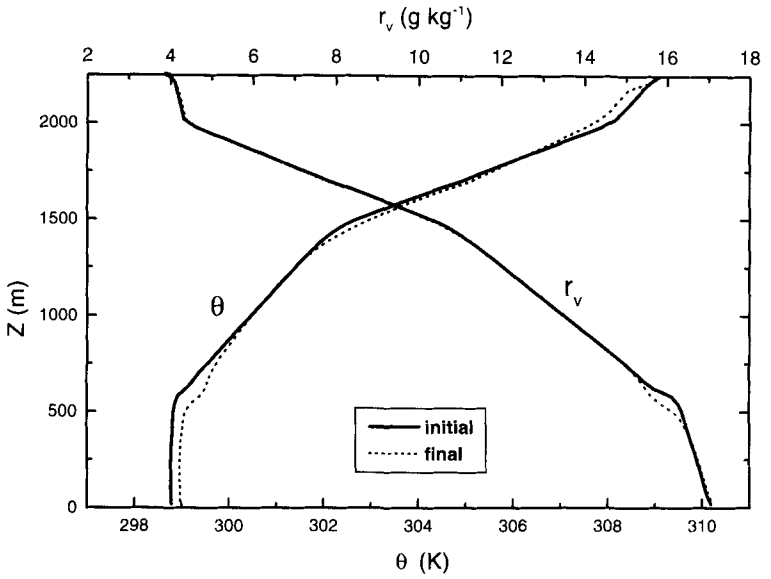

Figure 4. BOMEX shallow cumulus case as simulated by the single-column model: initial (solid) and modelled (dashed) profiles of θ and r_v (see text).

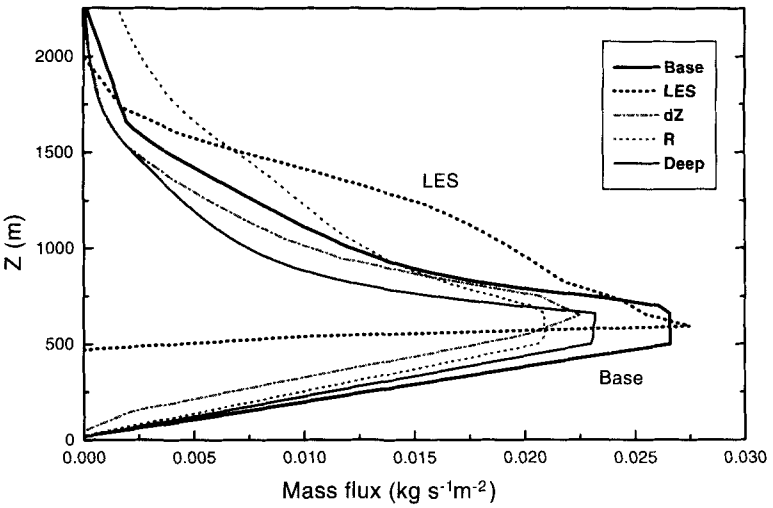

Figure 5. Nine-hour averaged convective mass-flux profiles for the BOMEX case. Comparison of large-eddy simulation results (thick dashed line) with different Meso-NH single-column model runs: baseline simulation (thick solid line), with vertical resolution of 100 m (dashed-dotted line), with cloud radius of 100 m (dotted line), and including convective downdraughts and precipitation (thin solid line).

6. Conclusions

We have presented a bulk mass-flux convection parametrization for deep and shallow convection that includes an efficient treatment of numerics, moist thermodynamics and convective downdraughts*.

* The corresponding computer code is available as an optimized portable routine in Fortran 90 on ftp://ftp.aero.obs-mip.fr/pub/salsa/becp/convect/

The scheme has been evaluated here in an SCM framework. Preliminary 3D tests of the scheme at different horizontal resolutions (10–200 km) have also been run with the global French NWP model ARPEGE (Courtier and Geleyn 1988) and the Meso-NH mesoscale model (Stein *et al.* 2000). Further tests are currently being conducted in the Canadian NWP and regional climate models. It was of course not possible to present all the test results in the context of the present manuscript. The results suggest that the present scheme provides reasonable solutions in terms of predicted rainfall and has a positive impact on predicted temperature and moisture biases in the Tropics and consequently on the cloud and radiation budget. The application of the scheme to various scales is supported by the use of a CAPE convective closure that assures a smooth interaction with the large-scale environment and efficiently suppresses CISK*-like spin-up processes on the grid-scale. Furthermore, to our knowledge it is the first time that a CAPE convective closure is also successfully applied to shallow convection.

We believe that the current version of the scheme contains the essential physics to parametrize the first-order effects of moist convection. However, one should be aware of several inherent shortcomings of schemes designed to parametrize convection. For example: (i) interactions between parametrized clouds are neglected, even in complex spectral schemes of the Arakawa–Schubert type; (ii) deep convective clouds are multiscale so that the scale separation necessarily imposed by parametrizations is artificial (Bretherton and Smolarkiewicz 1989; Mapes 1997); (iii) microphysics and the cloud–radiation interactions are very difficult to represent accurately with parametrized convective clouds, which are assumed to be in a steady-state condition (Betts 1997). These problems, in addition to the innate stochastic nature of convection, raise the question of whether it is possible to formulate convective parametrizations that are sufficiently general and accurate for long-range integrations. Considering the many uncertainties that still exist, it is likely that the overall performance of the present parametrization could be improved further, both by more refined calibration of existing parameters (e.g. precipitation efficiency) and by adding more layers of complexity to the scheme, e.g. allowing for multiple updraughts that differ by their characteristic cloud radius. Thus, we view the current version as a foundation upon which improved parametrization techniques can be built in a manner that is commensurate with our expanding understanding of convective activity, its interactions with larger-scale processes, and the constraints imposed by numerical models.

Currently the GCSS Working Groups 1 and 4 are addressing fundamental issues related to the convective parametrization problem by evaluating convection schemes against observational data and data from CRMs. Continued work on this problem is important because parametrized convection is likely to be an essential component of NWP models and GCMs for many years to come. This is true because, even as advances in computer power allow higher-resolution convective cloud-resolving model configurations to become viable for many tasks, high-resolution grids are likely to be limited in area and embedded within coarser-resolution domains (Stein *et al.* 2000). These outer domains will likely require a parametrization scheme in order to adequately represent convective effects and supply appropriate boundary conditions to the high-resolution grid. Thus, refined methods for convective parametrization may be essential elements in modelling systems even when modelling efforts focus on inner-domain grids where convection is explicitly resolved.

* Conditional instability of the second kind.

ACKNOWLEDGEMENTS

The first author would like to express all his gratitude to J. S. Kain from National Severe Storms Laboratory (Norman, Oklahoma) who was too modest to figure as a co-author, but his previous work and discussions with him were of invaluable help to us. J. F. Geleyn and P. Bougeault are thanked for their encouragement for this three-year project, as are S. Krueger, S. Lazarus and J. L. Redelsperger for making available the TOGA-COARE forcing data. Our special gratitude goes to Dominique Paquin, Celine Mari and Isabelle Mallet for providing numerous tests with the scheme, and to J. Duron for the development of the graphical software. Computer resources have been made available by Institut du Developpement et des Ressources Informatique Scientifique/Centre Nationale de la Recherche Scientifique and Météo France.

APPENDIX

Definition of latent and specific heats

The specific latent heats of vaporization, sublimation and melting as functions of temperature T are defined by

$$L_v(T) = L_v(T_t) + (C_{pv} - C_\ell)(T - T_t), \tag{A.1}$$

$$L_s(T) = L_s(T_t) + (C_{pv} - C_s)(T - T_t), \tag{A.2}$$

$$L_m(T) = L_s(T) - L_v(T), \tag{A.3}$$

with

$$T_t = 273.16\ \text{K}, \quad L_v(T_t) = 2.5008 \times 10^6\ \text{K J kg}^{-1}, \quad L_s(T_t) = 2.8345 \times 10^6\ \text{K J kg}^{-1}, \tag{A.4}$$

where the specific heats for phase change are in J kg^{-1}. The specific heat constants are defined as

$$C_{pv} = 4R_v\ \text{J kg}^{-1}, \quad C_\ell = 4.218 \times 10^3\ \text{J kg}^{-1}, \quad C_s = 2.106 \times 10^3\ \text{J kg}^{-1}, \tag{A.5}$$

with $R_v = 461.525\ \text{J kg}^{-1}\text{K}^{-1}$. The gas constant and specific heat for dry air are defined as $R_d = 287.06\ \text{J kg}^{-1}\text{K}^{-1}$ and $C_{pd} = 7/2R_d\ \text{J kg}^{-1}$, respectively.

REFERENCES

Alexander, G. D. and Cotton, W. R. 1998 The use of cloud resolving simulations of mesoscale convective systems to build a mesoscale parameterization scheme. *J. Atmos. Sci.*, **55**, 2137–2161

Anthes, R. A. 1977 A cumulus parameterization scheme utilizing a one-dimensional cloud model. *Mon. Weather Rev.*, **105**, 270–286

Arakawa, A. and Schubert, W. H. 1974 Interaction of a cumulus cloud ensemble with the large-scale environment: Part I. *J. Atmos. Sci.*, **31**, 674–701

Bechtold, P., Redelsperger, J. L., Beau, I., Blackburn, M., Brinkop, S., Grandpeix, J. Y., Grant, A., Gregory, D., Guichard, F., Hoff, C. and Ioannidou, E. 2000 A GCSS model intercomparison for a tropical squall line observed during TOGA-COARE. Part II: Intercomparison of SCMs with CRM. *Q. J. R. Meteorol. Soc.*, **126**, 865–889

Betts, A. K. 1997 The parameterization of deep convection. Pp. 255–279 in *The physics and parameterization of moist atmospheric convection*. Ed. R. K. Smith. NATO ASI Series Vol. C505. Kluwer Academic Publishers, Amsterdam, The Netherlands

Betts, A. K. and Miller, M. J. 1986 A new convective adjustment scheme. Part II: Single-column tests using GATE wave, BOMEX, ATEX, and arctic air-mass data sets. *Q. J. R. Meteorol. Soc.*, **112,** 693–709

Bolton, D. 1980 The computation of equivalent potential temperature. *Mon. Weather Rev.*, **108,** 1046–1053

Bougeault, P. 1985 A simple parameterization of the large-scale effects of cumulus convection. *Mon. Weather Rev.*, **113**, 2108–2121

Bretherton, C. S. and Smolarkiewicz, P. K. 1989 Gravity waves, compensating subsidence and detrainment around cumulus clouds. *J. Atmos. Sci.*, **46,** 740–759

Carpenter, R. L. Jr., Droegemeier, K. K. and Blyth, A. M. 1998 Entrainment and detrainment in numerically simulated cumulus congestus clouds. Part I: General results. *J. Atmos. Sci.*, **55,** 3433–3439

Charney, J. and Eliassen, A. 1964 On the growth of the hurricane depression. *J. Atmos. Sci.*, **21,** 68–75

Cohen, C. 2000 A quantitative investigation of entrainment and detrainment in numerically simulated cumulonimbus clouds. *J. Atmos. Sci.*, **57,** 1657–1674

Courtier, P. and Geleyn, J.-F. 1988 A global numerical weather prediction model with variable resolution: Application to the shallow-water equations. *Q. J. R. Meteorol. Soc.*, **114,** 1321–1346

Davies-Jones, R. P. 1983 An accurate theoretical approximation for adiabatic condensation temperature. *Mon. Weather Rev.*, **111,** 1119–1121

Donner, L. J. 1993 A cumulus parameterization including mass fluxes, vertical momentum dynamics, and mesoscale effects. *J. Atmos. Sci.*, **50,** 889–906

Emanuel, K. A. 1991 A scheme for representing cumulus convection in large-scale models. *J. Atmos. Sci.*, **48,** 2313–2335

1994 *Atmospheric convection.* Oxford University Press

Fritsch, J. M. and Chappell, C. F. 1980 Numerical prediction of convectively driven mesoscale pressure systems. Part I: Convective parameterization: *J. Atmos. Sci.*, **37,** 1722–1733

Fritsch, J. M., Houze, R. A., Adler, R., Bluestein, H., Bosart, L., Brown, J., Carr, F., Davies, C., Johnson, R. H., Junker, N., Kuo, Y.-H., Rutledge, S., Smith, J., Toth, Z., Wilson, J. W., Zipser, E. and Zrnic, D. 1998 Quantitative precipitation forecasting: Report of the eighth prospectus development team, U.S. weather research program. *Bull. Am. Meteorol. Soc.*, **79,** 285–299

Gregory, D. and Miller, M. J. 1989 A numerical study of the parameterization of deep tropical convection. *Q. J. R. Meteorol. Soc.*, **115,** 1209–1241

Gregory, D. and Rowntree, P. R. 1990 A mass-flux convection scheme with representation of cloud ensemble characteristics and stability dependent closure. *Mon. Weather Rev.*, **118,** 1483–1506

Grell, G. A. 1993 Prognostic evaluation of assumptions used by cumulus parameterizations. *Mon. Weather Rev.*, **121,** 764–787

Hu, Q. 1997 A cumulus parameterization based on a cloud model of intermittently rising thermals. *J. Atmos. Sci.*, **54,** 2292–2307

Kain, J. S. and Fritsch, J. M. 1990 A one-dimensional entraining/detraining plume model and its application in convective parameterizations. *J. Atmos. Sci.*, **47,** 2784–2802

1993 Convective parameterization for mesoscale models: The Kain–Fritsch scheme. *Meteorol. Monographs*, **46,** 165–170

Kershaw, R. and Gregory, D. 1997 Parameterization of momentum transport by convection. Part I: Theory and cloud modelling results. *Q. J. R. Meteorol. Soc.*, **123,** 1133–1151

Krueger, S. K., Gregory, D., Moncrieff, M. W., Redelsperger, J.-L. and Tao, W.-K. 1996 GCSS Working Group 4: First cloud-resolving model intercomparison project. Case 2. Technical Report. Meteorological Department, University of Utah

Kuo, H. L. 1965 On formation and intensification of tropical cyclones through latent heat release by cumulus convection. *J. Atmos. Sci.*, **22,** 40–63

Kuo, H. L. and Raymond, W. H. 1980 A quasi-one-dimensional cumulus cloud model and parameterization of cumulus heating and mixing effects. *Mon. Weather Rev.*, **108,** 991–1009

Lafore, J.-P., Stein, J., Asencio, N., Bougeault, P., Ducrocq, V., Duron, J., Fischer, C., Hereil, P., Mascart, P., Pinty, J.-P., Redelsperger, J.-L., Richard, E. and Vila-Guerau de Arellano, J. 1998 The Meso-NH atmospheric simulation system. Part I: Adiabatic formulation and control simulations. *Annales Geophysicae*, **16**, 90–109

Lin, C. and Arakawa, A. 1997 The macroscopic entrainment process of simulated cumulus ensemble. Part II: Testing the entraining-plume model *J. Atmos. Sci.*, **54**, 1027–1043

Manabe, S. and Strickler, R. 1964 Thermal equilibrium of the atmosphere with a convective adjustment. *J. Atmos. Sci.*, **21**, 361–385

Mapes, B. E. 1997 Equilibrium versus activation control of large-scale variations of tropical deep convection. Pp. 321–358 in *The physics and parameterization of moist atmospheric convection.* Ed. R. K. Smith. NATO ASI Series, Vol. 505. Kluwer Academic Publishers, Amsterdam, The Netherlands

Moncrieff, M. W., Gregory, D., Krueger, S. K., Redelsperger, J. L. and Tao, W. K. 1997 GEWEX Cloud System Study (GCSS) working group 4: Precipitating convective cloud systems. *Bull. Am. Meteorol. Soc.*, **78**, 831–845

Ogura, Y. and Cho, H.-R. 1973 Diagnostic determination of cumulus populations from large-scale variables. *J. Atmos. Sci.*, **30**, 1276–1286

Ooyama, K. 1971 A theory on parameterization of cumulus convection. *J. Meteorol. Soc. Jpn.*, **49**, 744–756

Raymond, D. J. 1995 Regulation of moist convection over the West Pacific warm pool. *J. Atmos. Sci.*, **52**, 3945–3959

Redelsperger, J. L. and Sommeria, G. 1986 Three-dimensional simulation of a convective storm: Sensitivity studies on subgrid parameterisation and spatial resolution. *J. Atmos. Sci.*, **43**, 2619–2635

Siebesma, A. P. 1998 Shallow cumulus convection. Pp. 441–486 in *Buoyant convection in geophysical flows.* Eds. E. J. Plate, E. E. Fedorovich, X. V. Viegas and J. C. Wyngaard. Kluwer Academic Publishers, Amsterdam, The Netherlands

Siebesma, A. P. and Cuijpers, J. W. M. 1995 Evaluation of parametric assumptions for shallow cumulus convection. *J. Atmos. Sci.*, **52**, 650–666

Simpson, J. 1983 Cumulus clouds: interactions between laboratory experiments and observations as foundations for models. Pp. 399–412 in *Mesoscale Meteorology.* Eds. D. K. Lilly and T. Gal-Chen. Reidel, Dordrecht, The Netherlands

Stein, J., Richard, E., Lafore, J.-P., Pinty, J.-P., Ascensio, N. and Cosma, S. 2000 Meso-NH simulations with grid-nesting and ice-phase parameterization. *Meteorol. Atmos. Phys.*, **72**, 203–221

Sun, W.-H. and Haines, P. A. 1996 Semi-prognostic tests of a new cumulus parameterization scheme for mesoscale modeling. *Tellus*, **48A**, 272–289

Tao, W.-K., Simpson, J. and McCumber, M. 1989 An ice-water saturation adjustment. *Mon. Weather Rev.*, **117**, 231–235

Tiedtke, M. 1989 A comprehensive mass flux scheme for cumulus parameterization in large-scale models. *Mon. Weather Rev.*, **117**, 1779–1800

Wang, J. and Randall, D. A. 1996 A cumulus parameterization based on the generalized convective available potential energy. *J. Atmos. Sci.*, **53**, 716–727

Warner, J. 1970 On steady-state one-dimensional models of cumulus convection. *J. Atmos. Sci.*, **27**, 1035–1040

Yanai, M., Esbensen, S. K. and Chu, J.-H. 1973 Determination of bulk properties of tropical cloud clusters from large-scale heat and moisture budgets. *J. Atmos. Sci.*, **30**, 611–627

Zhang, D.-L. and Fritsch, J. M. 1986 Numerical simulation of the meso-β scale structure and evolution of the 1977 Johnstown flood. Part I: Model description and verification. *J. Atmos. Sci.*, **43**, 1913–1943